Form-Finding and Stability Analysis of Tensegrity Structures using Nonlinear Programming and Fictitious Material Properties

***M. Ohsaki[1], J.Y. Zhang[2], and T. Taguchi[1]**

[1]Department of Architecture, Hiroshima University, Kagamiyama 1-4-1, Higashi-Hiroshima 739-8527, Japan.
[2]Department of Architecture and Urban Design, Nagoya City University, Japan

*Corresponding author: ohsaki@hiroshima-u.ac.jp

Abstract

An optimization approach is presented for form-finding of tensegrity structures. It is shown that various equilibrium shapes can be easily found by solving a forced-deformation analysis problem formulated as a minimization problem of the total strain energy. The self-equilibrium forces can be found from the optimality conditions of the nonlinear programming problem, and the stability is always guaranteed owing to local convexity of the strain energy. The equilibrium shape and self-equilibrium forces can be modified by assigning fictitious material properties of cables. The proposed approach is successfully applied to form-finding of a tensegrity tower.

Keywords: Tensegrity, Form-finding, Optimization, Stability

Introduction

Tensegrity structure consists of cables and struts that carry tensile and compressive forces, respectively. Self-equilibrium forces, or prestresses, are introduced to stabilize the structure. Since the shape of the structure defined by nodal coordinates at self-equilibrium state depends on the member forces, it is difficult to obtain a desired shape. Therefore, several analytical and numerical approaches have been developed for form-finding of tensegrity structures (Zhang and Ohsaki, 2006).

Miki and Kawaguchi (2010) proposed an approach to form-finding by solving an optimization problem. Gaspani et al. (2011) carried out form-finding analysis using nonlinear programming approach. Chen et al. (2012) used an ant-colony method for form-finding.

In this study, we present a method for form-finding of tensegrity structures using a nonlinear programming approach. Various equilibrium shapes are found by utilizing fictitious material properties. Stability of the self-equilibrium state is also discussed.

Basic Equations

Let N_i $(i = 1, \dots, m)$ denote the axial force of member i of a tensegrity structure consisting of m members in the 3-dimensional space. The vector consisting of coordinates of all n nodes is denoted by $\boldsymbol{X} \in \mathbb{R}^{3n}$. The unstressed length L_i^0 of member i is given. Then, the length $L_i(\boldsymbol{X})$ of i th member satisfying compatibility (connectivity) conditions at nodes is a function of $\boldsymbol{X}$, and its gradient $\nabla L_i(\boldsymbol{X})$ consists of directional cosines of members. If we neglect the self-weight, the equilibrium equation is written as

$$\sum_{i=1}^{m} N_i \nabla L_i(\boldsymbol{X}) = \boldsymbol{0} \tag{1}$$

Although the material of tensegrity structure is usually linear elastic, we use a fictitious material in the process of form-finding. For the given unstressed member lengths, the strain energy of member i is regarded as a function of $L_i(\boldsymbol{X})$, which is denoted by $S_i(L_i(\boldsymbol{X}))$. Then the total strain energy $S(\boldsymbol{X})$ is obtained as

$$S(\boldsymbol{X}) = \sum_{i=1}^{m} S_i(L_i(\boldsymbol{X})) \tag{2}$$

The self-equilibrium shape is found by solving an optimization problem. The variables are nodal coordinates $\boldsymbol{X}$, and the objective function is the total strain energy $S(\boldsymbol{X})$. When no constraint is given, the stationary condition of $S(\boldsymbol{X})$ is given as

$$\frac{\partial S(\boldsymbol{X})}{\partial X_i} = \sum_{i=1}^{m} \frac{\partial S_i(L_i(\boldsymbol{X}))}{\partial L_i} \nabla L_i(\boldsymbol{X}) = \boldsymbol{0}, \quad (i = 1, \ldots, 3n) \tag{3}$$

At the optimal solution satisfying Eq. (3), the equilibrium equation (1) is satisfied by regarding $\partial S_i / \partial L_i$ as the axial force N_i of member i.

This optimization problem is a standard analysis problem with forced deformation for satisfying the compatibility at nodes for specified unstressed member lengths. Furthermore, the total potential energy is equal to the total strain energy, because no external load is applied at the self-equilibrium state. Therefore, the principle of minimum total potential energy ensures stability of the equilibrium shape obtained by minimizing the strain energy; however, we use a fictitious material, rather than the true material, in this process of form-finding.

After obtaining $\boldsymbol{X}$ as the solution of the optimization problem, we assign the properties of the true material, and compute the true axial force $N_i^*(\boldsymbol{X})$ from the member lengths $L_i(\boldsymbol{X})$ at equilibrium and the unstressed length L_i^0. Then, the tangent stiffness matrix $\boldsymbol{K}^* \in \mathbb{R}^{3n\times 3n}$ using the true material is defined as the sum of the linear stiffness matrix $\boldsymbol{K}_{\mathrm{E}}^* \in \mathbb{R}^{3n\times 3n}$ and the geometrical stiffness matrix $\boldsymbol{K}_{\mathrm{G}}^* \in \mathbb{R}^{3n\times 3n}$ as

$$\boldsymbol{K}^* = \boldsymbol{K}_{\mathrm{E}}^* + \boldsymbol{K}_{\mathrm{G}}^* \tag{4}$$

The tangent stiffness matrix using fictitious material is denoted by $\boldsymbol{K} \in \mathbb{R}^{3n\times 3n}$. Let $\lambda_{\min}$ denote the lowest (7th) eigenvalue of $\boldsymbol{K}$ excluding six zero eigenvalues corresponding to rigid-body motions. The principle of minimum total potential energy ensures that $\lambda_{\min} > 0$ at the equilibrium state. Let $\hat{\boldsymbol{K}} \in \mathbb{R}^{3n\times 3n}$ denote the increment of $\boldsymbol{K}^*$ from $\boldsymbol{K}$; i.e.,

$$\boldsymbol{K}^* = \boldsymbol{K} + \hat{\boldsymbol{K}} \tag{5}$$

Define the nodal displacement vector $\boldsymbol{d} \in \mathbb{R}^{3n}$ as a linear combination of the eigenvectors $\boldsymbol{\Phi}_i \in \mathbb{R}^{3n}$ $(i = 7, \ldots, 3n)$ excluding rigid-body motions as

$$\boldsymbol{d} = \sum_{i=7}^{3n} \alpha_i \boldsymbol{\Phi}_i \tag{6}$$

where α_i $(i = 7, \ldots, 3n)$ are arbitrary coefficients that are not equal to 0 simultaneously. Since the equilibrium state using the fictitious material is stable, $\boldsymbol{d}^{\mathrm{T}} \boldsymbol{K} \boldsymbol{d} > 0$ holds. Therefore, the equilibrium state using the true material is stable if the following condition is satisfied:

$$\boldsymbol{d}^{\mathrm{T}}\hat{\boldsymbol{K}}\boldsymbol{d} \geq 0 \tag{7}$$

When the fictitious material is defined using a bilinear stress-strain relation with degrading stiffness, and the true material has constant stiffness that is equal to the initial stiffness of the fictitious material, then $\hat{\boldsymbol{K}}$ is positive semi-definite, and the condition (7) is satisfied. Note that this condition is a sufficient but not a necessary condition as demonstrated in the numerical examples.

We can also formulate a constrained optimization problem with upper bound $L_{J_i}^{\mathrm{U}}$ for cable J_i $(i = 1, \ldots, p)$ as

$$L_{J_i}(\boldsymbol{X}) - L_{J_i}^{\mathrm{U}} \leq 0, \quad (i = 1, \ldots, p) \tag{8}$$

The optimality condition for the minimization problem of $S(\boldsymbol{X})$ under constraint (8) is written as

$$\frac{\partial S(\boldsymbol{X})}{\partial X_i} = \sum_{i=1}^{m} \frac{\partial S_i(L_i(\boldsymbol{X}))}{\partial L_i} \nabla L_i(\boldsymbol{X}) + \sum_{i=1}^{p} \lambda_i \nabla L_{J_i}(\boldsymbol{X}) = \boldsymbol{0}, \quad (i = 1, \ldots, 3n) \tag{9}$$

Hence, the axial force of cable J_i should be equal to $\partial S_i / \partial L_i + \lambda_i$ to satisfy the equilibrium equation (1). Since $L_i(\boldsymbol{X})$ is not a convex function of $\boldsymbol{X}$, stability of the equilibrium shape using the fictitious material is not guaranteed, when constraints on member length are given.

Optimization is carried out using SNOPT Ver.7 (Gill et al., 2002) that is based on sequential quadratic programming (SQP). The sensitivity coefficients are computed analytically. When the approximate Hessian of Lagrangian is singular at a step of SQP, SNOPT stabilizes the QP subproblem by assigning small positive values on the diagonals of the Hessian, which leads to a penalty term of the quadratic norm of the increment of variables. Therefore, for the analysis problem of a free-standing tensegrity structure, the rigid-body motions are successfully excluded, and the nearest solution from the initial solution is obtained.

The algorithm of form-finding is summarized as follows:

1. Assign initial shape, unstressed lengths of members, and properties of fictitious material.
2. Solve the optimization problem to obtain the nodal coordinates at equilibrium.
3. Assign the properties of true material, and compute the axial forces at equilibrium and unstressed length using the true material.
4. Evaluate stability of the equilibrium shape.

Example of Tensegrity Tower

The proposed approach is applied to form-finding of a tensegrity tower that consists of struts, vertical cables, saddle cables, diagonal cables, and horizontal cables (Zhang and Ohsaki, 2008). An example of three-layer tower is shown in Fig. 1. Form-finding is carried out for a 20-layer tensegrity tower as shown in Fig. 2(a). The tower has three struts in each layer, and the radius and height of each layer are 1.0 m and 2.25 m, respectively. The units are omitted, in the following, for simple presentation of the results.

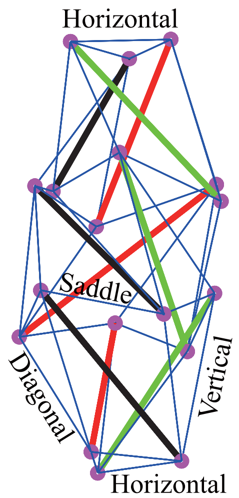

Figure 1. A 3-layer tensegrity tower model.

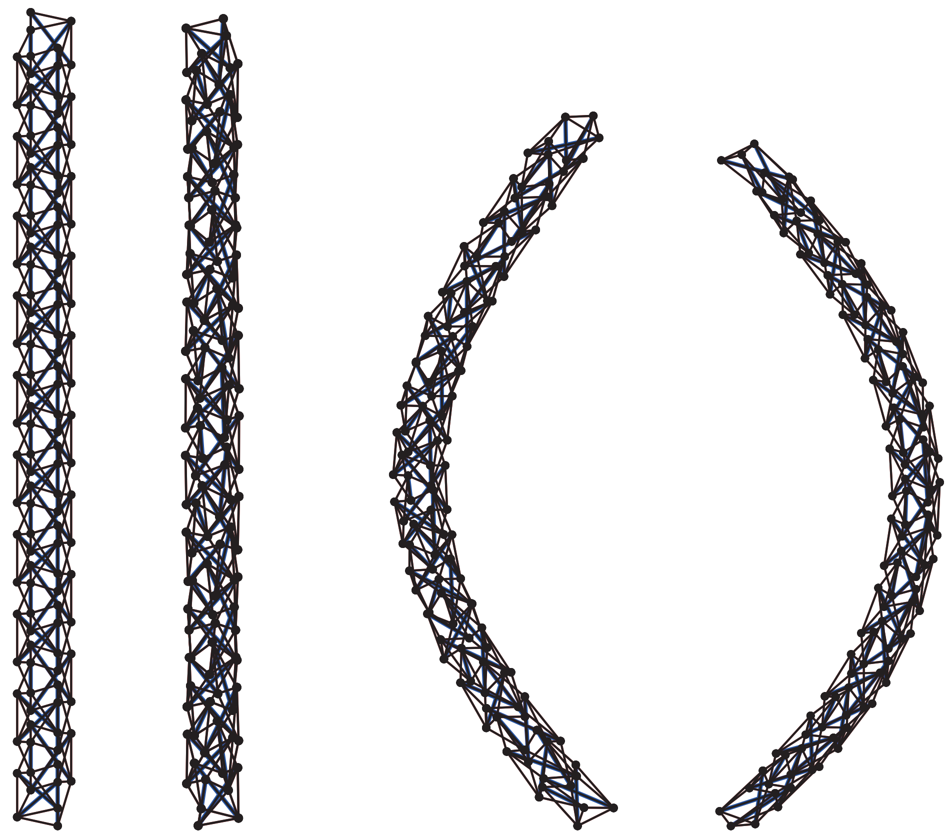

Figure 2. Initial and self-equilibrium shapes of a 20-layer tensegrity tower.

The unstressed lengths of cables and struts are assumed to be 80% and 100%, respectively, of the lengths of the members in the initial shape in Fig. 2(a). Let A_i and E_i denote the cross-sectional area and Young's modulus, respectively, of member i. The values of A_iE_i for the fictitious material are 100000 for struts and 1000 for cables. Note that the unstressed lengths of cables should be sufficiently smaller than the initial lengths in Fig. 2(a) to obtain a stable equilibrium shape, and to find various shapes that are not close to the initial shape.

Case 1:
The equilibrium shape obtained by solving the unconstrained optimization problem is shown in Fig. 2(b). The maximum axial force among all cables is 362.9. In Case 1, the stiffness of the true material is the same as that of the fictitious material. The axial forces are divided by 100 so that the absolute values of axial forces are in the order of 1/1000 of $A_i E_i$. Eigenvalue analysis is carried out for $\boldsymbol{K}^*$ to find that the 6th and 7th smallest eigenvalues as listed in Table 1. Since the 7th eigenvalue is sufficiently larger than the 6th eigenvalue that is approximately equal to 0, the equilibrium state is stable with six zero eigenvalues corresponding to rigid-body motions.

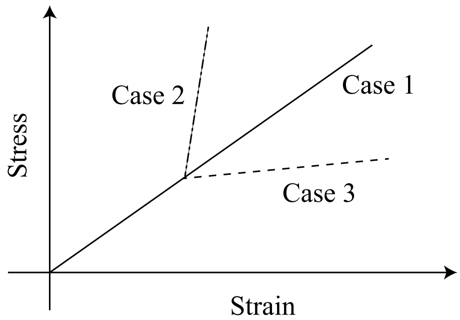

Figure 3. Bilinear stress-strain relations.

Case 2:
We next consider a fictitious material with bilinear stress-strain relation. The 60 vertical cables are classified into six groups connecting the nodes with the same *xy*-coordinates in the horizontal plane of the initial shape. Ten cables in one of six groups are selected to have the bilinear stress-strain relation as indicated as Case 2 in Fig. 3. The strain at the stiffness transition point is 0.1, and the value of $A_i E_i$ of the second part is $100 A_i E_i$. The equilibrium shape obtained by optimization is shown in Fig. 2(c). The minimum and maximum values of strains among the members with bilinear stress-strain relation are 0.1028 and 0.1030, which are close to 0.1. This way, a curved shape has been generated by assigning large stiffnesses for the cables that are vertically aligned at the initial shape.

We multiply 1/100 to axial forces of all members and carry out eigenvalue analysis of tangent stiffness matrix using the true material with constant stiffness $A_i E_i$ for all cables. The 6th and 7th eigenvalues are listed in Table 1, which shows that the structure is stable, although the true material has smaller stiffness than the fictitious material, and the sufficient condition (7) for stability is not satisfied. If we set the maximum member length $1.1 L_i^0$ and solve the constrained optimization problem, the same equilibrium shape as shown in Fig. 2(c) is obtained. The axial forces of the constrained members in layers 1, 3, and 5 are listed in Table 2, which confirms that the axial forces at equilibrium can be obtained as the sum of the differential coefficient $\partial S_i / \partial L_i$ and the Lagrange multiplier λ_i.

Table 1. Eigenvalues of tangent stiffness matrix using true material.

Case	6th	7th
1	6.135×10^{-8}	0.06125
2	-1.094×10^{-8}	0.02594
3	1.861×10^{-9}	0.02171

Table 2. Axial forces at equilibrium of constrained members in layers 1, 3, and 5.

Layer	Bilinear model	Constrained optimization		
		(A) Differential coefficient of strain energy	(B) Lagrange multiplier	(A) + (B)
1	397.6	100.0	300.1	400.0
3	380.2	100.0	282.6	382.6
5	380.8	100.0	283.2	383.2

Case 3:

Fictitious material property is given in the same vertical cables as Case 2. However, we decrease the value of $A_i E_i$ of the second part of the vertical cables to $A_i E_i / 100$ as indicated by Case 3 in Fig. 3. The equilibrium shape obtained by solving the unconstrained optimization problem is shown in Fig. 2(d). As seen from Figs. 2(c) and (d), the tower can be bent to opposite directions by increasing and decreasing the value of $A_i E_i$ of the vertical cables in the specified group. The axial forces of the vertical cables with bilinear stress-strain relation are between 103 and 104, which are close to the specified value $0.1 A_i E_i$. We multiply 1/100 to axial forces of all members and carry out eigenvalue analysis of tangent stiffness matrix. The 6th and 7th lowest eigenvalues are listed in Table 1, which confirms the stability of structure. Since the stiffness of the fictitious material is smaller than that of the true material, the equilibrium shape with the true material is stable, if the shape with fictitious material is stable.

Conclusions

The following conclusions have been obtained in this study:

1. Various equilibrium shapes can be obtained using the fictitios material with bilinear stress-strain relations. The equilibrium shape can be successfully found by solving an unconstrained optimization problem of minimizing the total strain energy.
2. A curved tensegrity tower can be generated by assigning fictitios materials for a group of vertically aligned vertical cables. It has been shown that the optimization problem with bilinear stress strain relation is equivalent to a constrained optimization problem with upper bound for the member lengths.
3. The equilibrium shape of the tensegrity structure is stable, if the stable equilibrium is found using a fictitious material with degrading bilinear stress-strain relation, and the true material has the constant stiffness that is equal to the initial stiffness of the fictitious material.
4. The rigid-body motions need not be constrained when solving the optimization problem using an SQP method, because the quadratic programming subproblem is automatically stabilized by assigning small positive values in the diagonals of the approximate Hessian of the Larangian.

References

Chen, Y, Feng, J. and Wu, Y. (2012) Novel form-finding of *tensegrity structures using ant colony systems, J. Mechanics and Robotics*, ASME **4**, No. 031001.

Gasparini, D., Klinka, K. K. and Arcaro V. F. (2011) A finite element for form-finding and static analysis of tensegrity structures, *J. Mechanics of Materials and Structures* **6**, 1239–1253.

Gill, P. E., Murray, W. and Saunders, M. A. (2002) SNOPT: An SQP algorithm for large-scale constrained optimization, *SIAM J. on Optimization* **12**: 979-1006.

Miki, M. and Kawaguchi, K. (2010) Extended force density method for form-finding of tension structures, *J. Int. Association for Shell and Spatial Structures* **51**, 291–303.

Zhang, J. Y. and Ohsaki. M. (2006) Adaptive force density method for form-finding problem of tensegrity structures, *Int. J. Solids and Structures* **43**, 5658–5673.

Zhang, J. Y. and Ohsaki, M. (2008) Numerical form-finding method for tensegrity tower, *Proc. IASS Symposium 2008*, Int. Assoc. for Shell and Spatial Struct., Acapulco, Mexico.